

Liquid-liquid coexistence in the phase diagram of a fluid confined in fractal porous materials.

V. De Grandis, P. Gallo, and M. Rovere*

*Dipartimento di Fisica, Università "Roma Tre",
and Democritos National Simulation Center, INFN-CNR,
Via della Vasca Navale 84, 00146 Roma, Italy.*

Multicanonical ensemble sampling simulations have been performed to calculate the phase diagram of a Lennard-Jones fluid embedded in a fractal random matrix generated through diffusion limited cluster aggregation. The study of the system at increasing size and constant porosity shows that the results are independent from the matrix realization but not from the size effects. A gas-liquid transition shifted with respect to bulk is found. On growing the size of the system on the high density side of the gas-liquid coexistence curve it appears a second coexistence region between two liquid phases. These two phases are characterized by a different behaviour of the local density inside the interconnected porous structure at the same temperature and chemical potential.

PACS numbers: 61.20.Ja, 61.20.-p, 64.70.Fx

I. INTRODUCTION

The effect of confinement on the phase diagram of fluids is a longstanding problem with a wide interest from the theoretical point of view and a wide area of possible applications such as catalysis, adsorption and filtration. A large phenomenology on this subject can be found¹. Real porous materials show generally a complex structure made of an interconnected network of pores. Vycor glass and silica gels are relevant examples. It is important to distinguish between two classes of systems. In hosting media with very high porosity like silica aerogel (90% – 98%) it has experimentally been observed that the gas-liquid transition is preserved although the confinement causes a reduction of the critical temperature and a shrinkage of the gas-liquid coexistence curve^{2,3}. In mesoporous materials with a porosity in the range between 30% and 60%, as for instance Vycor glass, there are not direct observations of equilibrium phase transitions⁴. This last behaviour is predicted by theoretical work performed in the framework of lattice gas models^{1,4,5,6,7,8,9}. This type of approach is connected to the more general issue of the effects of quenched disorder on critical phenomena^{10,11,12,13,14}. In dilute silica aerogels with high porosity, however, phase transitions between equilibrium phases cannot be theoretically excluded^{15,16} although more recent experiments^{17,18} and mean field calculations^{8,9} questioned the early experimental findings of a gas-liquid transition in ⁴He in aerogel.

For dilute silica aerogels off lattice liquid state models have been introduced^{19,20} to take into account more in detail the microstructure of the confining systems. In these off lattice models the disordered porous material is modeled as a system of spheres frozen in a predefined structure. The quenched matrix approximately accounts for the geometric constraints of the interconnected pore structure of the solid. From both computer simulations^{20,21} and integral equation methods¹⁵ it has been found that the phase diagram of these models can show,

besides the gas-liquid coexistence (GLC), the presence of a second transition. This transition can be a gas-gas or a liquid-liquid coexistence depending on the liquid-matrix type of interaction. Nonetheless the appearance of this coexistence and its details depend on the way in which the confining random matrix is realized²². Moreover relevant wetting or drying effects could be present²⁰.

Therefore while the coexistence of different fluid forms in a simple monatomic fluid confined in silica aerogels is of uttermost interest, its existence is still a controversial result. The fact that the phase diagram has shown to depend so much on the details of the quenched random matrix has precluded so far more detailed microscopic analysis on these confined fluids and a systematic study of size effects.

From these considerations and a more recent theoretical analysis based on integral equation methods¹⁶ it emerges the importance of realizing by computer simulation an host system which accounts microscopically for the high porosity and the fractal structure of the silica aerogel. Its structure is due to the process of formation of the gel through the random aggregation of the silica particles and it is measured in small angle scattering experiments where a fractal dimension of $D = 1.8$ has been estimated^{23,24,25}. These microscopic features are not present in any of the previous lattice or off lattice simulated systems, mentioned above.

In order to build up a confining medium with the structure of silica aerogels, we have implemented a numerical procedure²⁶ based on the diffusion limited cluster-cluster aggregation (DLCA)^{23,24,25}. It has been shown^{23,24,25} that the DLCA algorithm is able to reproduce the structure factor and the fractal dimension of silica aerogels. In a previous study we calculated with the Multicanonical Ensemble Sampling (MES)^{27,28,29} the phase diagram of a Lennard-Jones fluid confined in the matrix generated with the DLCA and we found a GLC curve²⁶ and no evidence of a second transition except for a possible signature in a shouldering on the liquid side of the coexistence curve of a liquid-liquid coexistence (LLC). As it

is well known for aerogels²⁴ systems with the same porosity show the same average size of the clusters, the same connectivity, the same behaviour and range of the fractal scale. We expect therefore that performing simulations with confining media at constant porosity and increasing size that the behaviour of the liquid will be independent from the details of the realization of the matrix apart for the size effects themselves since the liquid is embedded in self similar structures.

In this paper we report the results obtained by increasing the size of the confining medium at constant porosity with the aim of inquiring about the existence of a LLC in the Lennard-Jones simple fluid possibly hidden in our past study by the small size of the simulated system.

II. SIMULATION DETAILS

To generate the off lattice matrix in a simulation box of side L we introduce a number N_s of spheres of diameter σ_s randomly placed and apply periodic boundary conditions. After the application of the DLCA algorithm the final configuration of the matrix consists of a percolated cluster of N_s spheres. For our former system, which we will call in the following system I²⁶, we used $L = 15\sigma_s$ and $N_s = 515$ in order to have a volume fraction $\eta = 0.08$ corresponding to a porosity $P = 92\%$. For the system simulated in the present work, system II, we fix the same η and porosity increasing the box length to $L = 20\sigma_s$. In this case the system consists of $N_s = 1222$ spheres. The average cluster size is $4\sigma_s$ independent from the system size. The particles of the confined fluid interact with a Lennard-Jones potential with $\sigma = \sigma_s$ at variance with real systems where the aerogel spheres are much larger than the fluid particles. In the following Lennard-Jones units will be used. The potential is truncated at $r_c = 2.5$. The interaction between the matrix spheres and the fluid particles is represented by a hard sphere potential with diameter σ . The simulation of the phase diagram of the confined fluid is performed by Monte Carlo in the grand canonical ensemble (GCMC) with the algorithm introduced by Wilding^{28,29}. By varying the chemical potential μ at constant temperature T we follow the behaviour of the density fluctuations and calculate the density distribution functions (DDF) $P(\rho)$. In a two phase region the DDF develop a double peak structure. The coexistence point between the two phases is located with the Wilding criterion²⁹ by tuning the chemical potential at constant temperature to obtain equal area under the two peaks. In the subcritical region where a large free energy barrier is present between the two phases the MES^{27,28,29} has been implemented to enhance the sampling of the two coexisting phases.

From the double peaked DDF we can extrapolate the biased sampling function at different chemical potentials and temperatures by means of the histogram reweighting technique³⁰. With the bias sampling function the MES can be carried on. In the final step the bias must be sub-

tracted to recover the real distribution function²⁶. To equilibrate system II 10^8 Monte Carlo moves have been generated, while equilibrium properties have been calculated with $10^9 - 10^{10}$ Monte Carlo moves. The system has been investigated in the range of temperatures from $T = 0.95$ to $T = 0.825$.

III. DENSITY DISTRIBUTION FUNCTIONS AND PHASE DIAGRAM

In Fig. 1 the bimodal DDF of system II are reported in the thermodynamical range where the MES analysis has been performed. The low density peaks corresponding to the gas phase show a behaviour very similar to the corresponding quantities in system I therefore the gas branch of the coexistence curve appears as almost independent from the size of the system. On the liquid side coexisting with the gas we observe instead large differences in the structure of the peaks. In system I they were found to be broad and asymmetric²⁶. Now in system II the form of the peaks is symmetric and sharper. To be more precise for temperatures $T < 0.90$ the density fluctuations are of the order of 0.07 in system I and 0.006 in system II in the same range of temperature variation $\Delta T \simeq 0.075$. By increasing the chemical potential at values above the

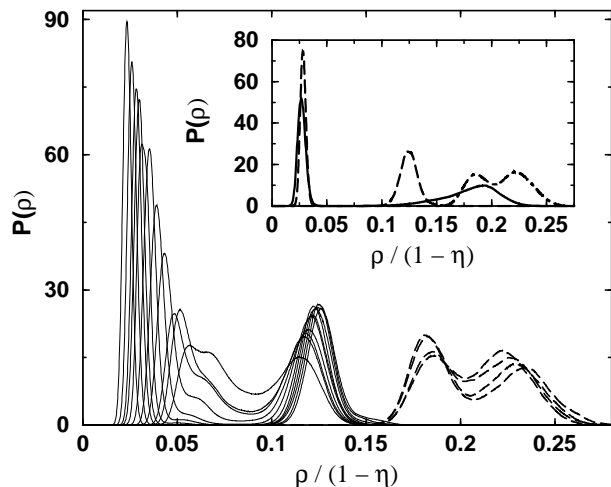


FIG. 1: Density distribution functions (DDF) of the fluid at the gas-liquid coexistence (solid line) for system II in the range of temperatures below the critical point from $T = 0.825$ to $T = 0.95$ and liquid-liquid coexistence (long-dashed lines) in the range of temperatures from $T = 0.825$ to $T = 0.85$. DDF with closer peaks correspond to higher temperatures. In the inset $P(\rho)$ of the liquid-gas coexistence in system I (solid line) compared with the liquid-gas (long-dashed line) and the liquid-liquid (dot-dashed line) distribution functions of system II at $T = 0.85$.

liquid-gas coexistence we find in the adsorption isotherms the appearance of a second coexistence in system II. The corresponding DDF are also reported in Fig. 1 where they

show very well defined peaks. In the inset of Fig. 1 it is shown how the bimodal $P(\rho)$ in the system I at $T = 0.85$ is modified in system II with the emerging of new structures. While the low density peak corresponding to the gas phase remains in the same position in system II, the liquid peak of system I splits in two in the larger simulation box disclosing the presence of a possible LLC. The new bimodal structure is obtained by increasing of 2% the value of the chemical potential from the value at the gas-liquid coexistence. The size of system I was not enough large to allow the resolution of the different contributions to the density fluctuations in the system in the region of the liquid peak.

From the peak positions of the DDF with the Wilding criterion the coexistence curves of system II have been determined and reported in Fig. 2 where they are compared with the coexistence curves of system I and with the bulk.

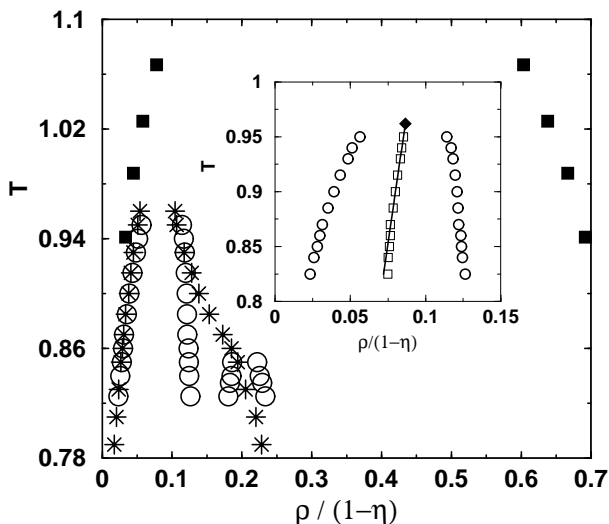


FIG. 2: Phase diagram of system II (open circles) compared with the one of system I (stars) and a portion of the bulk liquid-gas coexistence curve (filled squares). In the inset liquid-gas coexistence curve of system II (open circles) with the diameter (open squares) and the best fit to the rectilinear diameter law (solid line), the filled diamond represents the critical point obtained by extrapolation of the fit.

The confinement causes a substantial shrinkage of the gas-liquid coexistence curve and a shift toward lower temperatures and densities of the critical point. The confinement also does not induce large changes with respect to the gaseous phase of bulk fluid, in fact the gas branch of the gas-liquid coexistence curve in confinement almost coincides with the analogous branch in the bulk. On the liquid side of system II a new coexistence curve is now observed between a low density liquid, which we shall call liquid I, and an high density liquid, liquid II. We note that the range of extension of the phase diagram of the confined system is not quite affected by the system size. We checked that our results are independent from the

matrix realization by performing simulations with other two different matrices generated with DLCA at the same porosity and $L = 20$.

In system II, where the GLC appears as a well defined curve, it is possible to extrapolate the critical point position with the use of the law of the rectilinear diameter and the scaling law of the density³¹. In the inset of Fig. 2 we show the coexistence diameter $\rho_d = (\rho_g + \rho_l)/2$. The best fit to the rectilinear diameter law $\rho_d = \rho_c + A(T_c - T)$ combined with the scaling law $\rho_l - \rho_g = B(T_c - T)^\beta$ gives the following estimates of the liquid-gas critical parameters: $T_c = 0.96$ and $\rho_c = 0.0791$ to be compared with the values for the bulk $T_c = 1.1876$ and $\rho_c = 0.3197$ ²⁸. At variance with experimental results² we find a shift of the critical point to a lower density, this is due to the assumption of a pure repulsion between the fluid and the matrix¹⁵. The exponent β compatible with these critical values is in the range $0.30 \sim 0.32$ to be compared with the universal exponent $\beta = 0.3258$ found in the bulk²⁸. This also confirms the experimental finding that the universal behaviour of the gas-liquid transition in the bulk persists also in confinement^{2,3}.

IV. LIQUID-LIQUID COEXISTENCE REGION

In Fig. 3 we report the snapshots of two coexisting configurations of the fluid at $T = 0.85$ in the region of the second coexistence curve. From the snapshots we can observe that both liquid I and II are characterised by the presence of a large cluster and a number of smaller clusters with few particles. We calculated the gyration

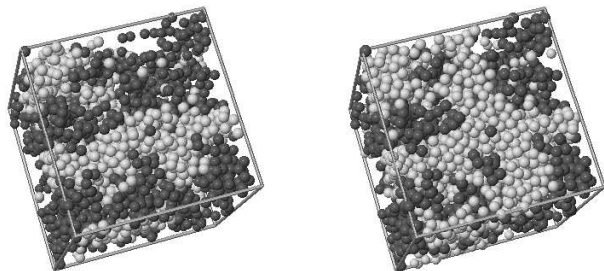


FIG. 3: Snapshots of the configurations of the confined fluid at $T = 0.85$ in the low density liquid phase (liquid I) on the left and in the high density liquid phase (liquid II) on the right. The gray and the black spheres represent the gel and the liquid particles respectively.

radius R_g of the larger cluster in the two liquid phases in the range of temperature from $T = 0.850$ to $T = 0.825$. R_g is defined by $R_g = \sqrt{\sum_i r_{ci}^2 / N}$, where r_{ci} is the distance between the particle i and the center of mass of the cluster. In liquid I we have an increase of number of particles in the system upon increasing temperature and a 3% increase in the number of particles corresponds to a 2.2% increase of the particles in the cluster and to a 7.3%

increase of the gyration radius. In liquid II we observe the opposite trend instead, an increase of number of particles is observed upon decreasing temperature. Besides a 5% increase in the number of particles corresponds to a 7% increase of the particles in the cluster while R_g grows only for an 1.7%.

The radial distribution functions (RDF) of the fluid in the two liquid phases (Fig. 4) have been also calculated with a canonical MC starting from equilibrated configurations obtained from the GCMC.

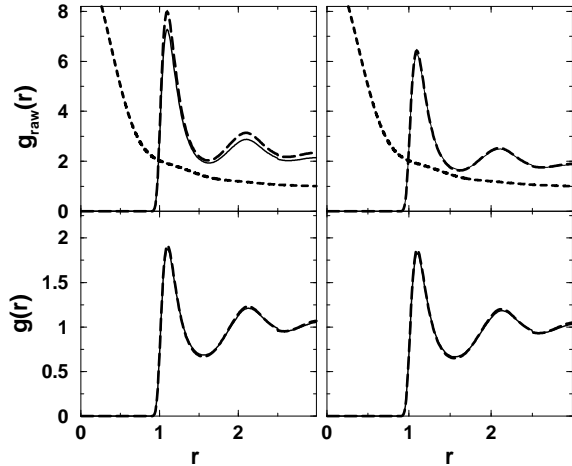


FIG. 4: Radial distribution functions of the fluid in the two phases, liquid I on the left, liquid II on the right, for $T=0.850$ (solid line), $T=0.825$ (long-dashed line). In the upper panels the RDF as obtained from simulation are shown together with the excluded volume correction (dashed line). In the lower panels the RDF are shown after the correction is applied.

The usual algorithm for obtaining the RDF from simulation consists in normalizing the number of atom pairs in a spherical shell with the uniform distribution of ideal particles in the same shell. Two of the $g_{raw}(r)$ functions obtained with this procedure are reported as an example in the upper panels of Fig. 4 for the less dense liquid, liquid I, and for the denser liquid, liquid II. According to previous literature³² when a fluid is confined the corrected RDF can be generated by appropriately normalizing $g_{raw}(r)$ with the *uniform* radial distribution function $g_u(r)$ which depends on the geometry of the confining medium and a factor $f = V/V_{eff}$ that accounts for the effective volume occupied by the particles: $g(r) = g_{raw}(r)/(f \cdot g_u(r))$. The function $g_u(r)$ can be determined with a convolution of the structure factor of the aerogel system and the internal structure factor of the single hard sphere³². The resulting $g_u(r)$ is reported in the upper panels of Fig. 4. The factor f and V_{eff} can

be empirically determined by imposing that $g(r)$ goes to 1 for large r . For liquid I the factor f decreases and V_{eff} increases with increasing temperature, in the two cases reported in Fig. 4, $f = 2.03$ for $T = 0.850, N = 1367$ and $f = 2.18$ for $T = 0.825, N = 1329$. In the case of liquid II, in Fig. 4 are reported $T = 0.850, N = 1634$ and $T = 0.825, N = 1717$, for which we get approximately the same value $f = 1.81$, independent from the temperature.

V. CONCLUSIONS

With the use of the DLCA algorithm to build a confining structure with fractal character we have found that the behaviour of the confined fluid confined in a fractal structure does not depend on the matrix realizations and finite size effects can be studied more systematically. By increasing the size of the simulation box the gas-liquid transition is well characterized, while a second coexistence curve appears on the high density side of the gas-liquid binodal curve. It is shown that in the low density liquid phase (liquid I) the size of the liquid domains increase with increasing temperature and equivalently the effective volume occupied by the particles V_{eff} grows. In the high density liquid phase (liquid II) instead there is no increase of the size of the liquid domains and of the effective volume. In this regime we have an increase of the local density which is made possible by little rearrangements of the particles. Even if drying effects due to the repulsive interaction between the fluid and the substrate cannot be excluded it seems that the high porous open structure of the aerogel network, built in our simulation, allows the formation of an almost homogeneous liquid phase inside the free volume.

The interpretation of fluid adsorption phenomena in aerogels is still controversial. In our simulation we studied equilibrium phase transitions and we did not consider hysteretic behaviour. In this respect our treatment is analogous to the integral equation study of Krakoviack et al.¹⁶, where a gas-liquid transition (but not a liquid-liquid one) is found for a fluid adsorbed in a high porosity aerogel. Calculations performed with mean field density functional theory aimed to study nonequilibrium behavior show instead a different scenario. The disordered character of the aerogel structure modifies the adsorption-desorption mechanism although at high temperatures there are indications of a gas-liquid transition^{8,9}. We need future experimental and theoretical work to get a more complete understanding of this vast and important phenomenology of fluid adsorption phenomena. In this respect computer simulation with complete finite size scaling analysis seems to be necessary since we have shown here that finite size effects are quite relevant.

* Author to whom correspondence should be addressed: rovere@fis.uniroma3.it

¹ Gelb L. D., Gubbins K. E., Radhakrishnan R. and

- Sliwiska-Bartkowiak M., Rep. Prog. Phys. **62**, 1573 (1999).
- ² Wong A. P. Y. and Chan M. H. W., Phys. Rev. Lett. **65**, 2567 (1990).
- ³ Wong A. P. Y., Kim S. B., Goldburg W. I. and Chan M. H. W., Phys. Rev. Lett. **70**, 954 (1993).
- ⁴ Monette L., Liu A. J. and Grest G. S., Phys. Rev. A **46**, 7664 (1992).
- ⁵ Kierlik E., Monson P. A., Rosinberg M. L., Sarkisov L. and Tarjus G., Phys. Rev. Lett. **87**, 055701 (2001).
- ⁶ Sarkisov L. and Monson P. A., Phys. Rev. E **65**, 011202 (2001).
- ⁷ Woo H.-J. Monson P. A., Phys. Rev. E **67**, 041207 (2003).
- ⁸ Detcheverry F., Kierlik E., Rosinberg M. L. and Tarjus G., Phys. Rev. E **68**, 061504 (2003).
- ⁹ Detcheverry F., Kierlik E., Rosinberg M. L. and Tarjus G., Phys. Rev. E **72**, 051506 (2005).
- ¹⁰ Brochard F. and de Gennes P. G., J. Phys. (France) Lett. **44**, 785 (1983); de Gennes P. G. J. Phys. Chem. **88**, 6469 (1984).
- ¹¹ Imry Y. and Ma S.-k., Phys. Rev. Lett. **35**, 1399 (1975).
- ¹² Fisher D. S., Grinstein G. M. and Khurana A., Phys. Today **41**, 56 (1988).
- ¹³ Maritan A., Swift M. R., Cieplak M., Chan M. H. W., Cole M. W. and Banavar J. R., Phys. Rev. Lett. **67**, 1821 (1991).
- ¹⁴ Cieplak M., Maritan A., Swift M. R., Toigo F., and Banavar J. R., Phys. Rev. E **66**, 056124 (2002).
- ¹⁵ Rosinberg M. L. in *New Approaches to Problems in Liquid State Theory*, edited by Caccamo C., Hansen J. P. and Stell G., Kluwer Academic, Dordrecht, 1999, p. 245.
- ¹⁶ Krakoviack V., Kierlik E., Rosinberg M. L. and Tarjus G., J. Chem. Phys. **115**, 11289 (2001).
- ¹⁷ Herman T., Day J. and Beamish J., Phys. Rev. B **72**, 184202 (2005).
- ¹⁸ Lambert T., Gabay C., Puech L. and Wolf P. E., J. Low. Temp. Phys. **134**, 293 (2004).
- ¹⁹ Madden W. G. and Glandt E. D., J. Stat. Phys. **51**, 537 (1988); Madden W. G., J. Chem. Phys. **96**, 5422 (1992).
- ²⁰ Page K. S. and Monson P. A., Phys. Rev. E **54** R9 and 6557 (1996).
- ²¹ Sarkisov L. and Monson P. A., Phys. Rev. E **61**, 7231 (2000).
- ²² Alvarez M., Levesque D. and Weis J. J., Phys. Rev. E **60** 5495 (1999).
- ²³ Hasmy A., Foret M., Pelous J. and Jullien R., Phys. Rev. B **48**, 9345 (1993).
- ²⁴ Hasmy A., Anglaret E., Foret M., Pelous J. and Jullien R., Phys. Rev. B **50**, 6006 (1994).
- ²⁵ Hasmy A., Vacher R. and Jullien R., Phys. Rev. B **50**, 1305 (1994).
- ²⁶ De Grandis V., Gallo P. and Rovere M., Phys. Rev. E **70**, 061505 (2004).
- ²⁷ Berg B. A. and Neuhaus T., Phys. Rev. Lett. **68**, 9 (1992).
- ²⁸ Wilding N. B., Phys. Rev. E **52**, 602 (1995).
- ²⁹ Wilding N. B., Am. J. Phys. **69**, 1147 (2001).
- ³⁰ Ferrenberg A. M. and Swendsen R. H., Phys. Rev. Lett. **61** 2635 (1988); **63**, 1195 (1989).
- ³¹ Rowlinson J. S. and Swinton F. L., *Liquids and Liquid Mixtures*, Butterworths, London, 1982.
- ³² Soper A. K., J. Phys. Condens. Matter **9** 2399 (1997).